Detecting Dwarf Galaxies Around NGC 55

Jonah Medoff,[1] Alex Drlica-Wagner,[1,2] Burçin Mutlu-Pakdil,[3] and Jeff Carlin[4]
[1)]*Department of Astronomy and Astrophysics, University of Chicago, Chicago, IL 60637, USA*
[2)]*Fermi National Accelerator Laboratory, P. O. Box 500, Batavia, IL 60510, USA*
[3)]*Department of Physics and Astronomy, Dartmouth College, Hanover, NH 03755, USA*
[4)]*Vera C. Rubin Observatory/AURA, 950 N Cherry Ave, Tucson, AZ 85719 USA*

In order to improve our understanding of the satellite populations of low-mass galaxies, the DECam Local Volume Exploration (DELVE) – DEEP Survey is performing a search for satellites around the isolated, low-mass galaxy, NGC 55. As part of this search, we characterize our dwarf galaxy detection sensitivity by injecting artificial dwarf galaxies into our data set and measuring the fraction that we can recover. Additionally, we inject and recover artificial dwarfs to test how the blending of resolved stars affects the detection of dwarf galaxies. We inject 650 artificial dwarfs across 26 DELVE-DEEP coadded images of the NGC 55 halo and use the software tool, Source Extractor, to perform source recovery. A dwarf-search pipeline is then run on our dwarf-injected catalogs, utilizing the `photutils` function, `find_peaks`, and detections are recorded as a function of dwarf size and luminosity. Our results demonstrate that we are most sensitive to large, bright dwarf galaxies, and our sensitivity begins to decrease as we approach DELVE-DEEP's detection limit or blending causes significant reductions in recovered magnitude. We also find that our results are hindered by the limitations of star-galaxy separation applied to distant, faint sources, which is possibly a consequence of the blending of small star clusters within dwarf galaxies.

I. INTRODUCTION

The ΛCDM model predicts the existence of faint dwarf galaxies orbiting both large host galaxies, like the Milky Way, and smaller hosts like the Magellanic Clouds (MC). These dwarf galaxies are the most ancient, chemically pristine, and dark-matter-dominated galaxies in the Universe, therefore studying them can shed light on the formation of the first galaxies, the evolution of host galaxies, as well as the abundance and distribution of dark matter.[1] Within the last 10-20 years, searches around the Milky Way halo have revealed dozens of dwarf galaxy satellites.[2,3] Conversely, the satellite populations around smaller, low-mass host galaxies are poorly understood from both a theoretical and observational perspective. Since it is difficult to distinguish MC satellites and Milky Way satellites, we must search for satellites specifically around isolated, low-mass hosts in the Local Universe. In recent years, several dwarf galaxies have been discovered around such hosts, such as the NGC 3019 satellite, Antlia B,[4] and the NGC 2403 and NGC 4214 satellites, MADCASH J074238+652501-dw and MADCASH J121007+352635-dw.[5,6] Despite these discoveries, a complete measurement of the satellite population of an MC-mass galaxy has yet to be performed.

Our goal, as part of the DELVE-DEEP Survey,[7] is to search for dwarf galaxy satellites of the nearby, low-mass galaxy, NGC 55, and produce the first complete satellite luminosity function for this galaxy down to an unprecedented limit of $M_V \sim -7$. An initial dwarf search was performed within the NGC 55 halo, although no clear dwarf galaxy candidates were detected. In order to better understand the sources that were detected, we performed artificial star tests on the DELVE-DEEP NGC 55 data in order to determine the completeness of our photometry. These artificial star tests alone, however, are not enough to determine how well we can actually detect dwarf galaxies. In order to characterize our dwarf detection sensitivity, we inject artificial dwarf galaxies into our data set and attempt to recover them. Additionally, we explore the blending of resolved stars that results as a consequence of source recovery and how this affects the recovered magnitudes of injected dwarf galaxies.

II. DELVE-DEEP SURVEY

The DELVE-DEEP Survey performs 135 deg^2 of deep imaging in the g and i bands around four isolated, Magellanic-sized galaxies in the Local Volume: NGC 55, NGC 300, Sextans B, and IC 5152. The main target of this project, NGC 55, is located at ∼2 Mpc and closely resembles the Large Magellanic Cloud in terms of both mass and morphology. DELVE-DEEP aims to be sensitive to resolved stars $\gtrsim 1.5$ mag below the tip of the red-giant-branch, enabling the detection of satellite galaxies up to $M_V \sim -7$.[7] Additionally, ΛCDM simulations predict 5-17 satellite galaxies around these four hosts in total,[8,9] so just around NGC 55, we could expect to discover up to 5 dwarf satellites.

III. DWARF INJECTION AND RECOVERY

We wish to determine our dwarf detection sensitivity as a function of size, measured as the log of the half-light radius in parsecs ($\log(r_h)$), and luminosity, measured in V-band absolute magnitude (M_V). Our artificial dwarf galaxies cover a parameter space of $-6.5 \geq M_V \geq -9$ and $2 \leq \log(r_h) \leq 3$, since we expect dwarfs brighter than $M_V = -9$ to be detected with 100% efficiency and dwarfs fainter than $M_V = -6.5$ to be completely undetectable. Known dwarfs with $-6.5 \geq M_V \geq -9$ tend to have half-light radii between 100 and 1000 pc.[1] Additionally, our artificial dwarf galaxies were randomly assigned position angles between $0 \leq PA \leq 180$ and ellipticities between $0 \leq e \leq 0.7$, since we expect galaxies with $e > 0.7$ to be undetectable due to overcrowding of resolved stars.

A total of 650 artificial dwarfs were injected across 26 DELVE-DEEP NGC 55 coadded images of varying exposure time and limiting magnitude. 25 dwarf galaxies were distributed randomly across each coadd, but with precautions to ensure that no dwarf overlapped with the edge of the image or with another dwarf. In order to increase the accuracy of our measured detection sensitivity, we would ideally inject $\sim 10^3 - 10^4$ artificial dwarfs, so it is likely that we will inject and recover more dwarfs in the future.

Each artificial dwarf galaxy's stellar population was sampled from an isochrone modeling a galaxy at distance D $\approx$ 2Mpc with an age of 10 Gyr and metallicity of [Fe/H] $= -2$ and generated according to a Salpeter IMF following $dN/dM \propto M^{-2.35}$,[10] which corresponds to what we would expect for an NGC 55 satellite. Each dwarf's stellar population was divided into resolved stars, defined as those with i-band mag ≤ 27, and unresolved stars, those with i-band mag > 27. The resolved stars were created as point sources convolved by the observed PSF and distributed according to an exponential profile, while the unresolved stars were modeled with a single Sérsic galaxy profile, whose flux was the sum of the individual unresolved stellar fluxes and position was the mean position of the resolved stars. Both the point sources, which were modeled with Delta Function profiles, and Sérsic profiles were generated using the galaxy image simulation package, `galsim`.[11] Each artificial dwarf was injected in both the g and i bands, after which all 26 coadds, in both g and i, were run through Source Extractor[12] for recovery. An example of an injected dwarf galaxy with its corresponding recovered stars is given by Figure 1. The recovered magnitudes for each star were measured using `MAG_PSF`, since we expect this to be the most accurate measure of magnitude for stars modeled with PSFs.

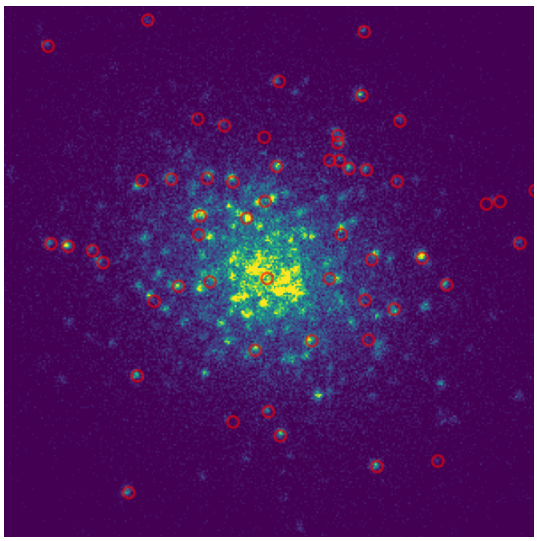

FIG. 1. Image of an artificial dwarf galaxy injected into one of DELVE-DEEP's NGC 55 coadds. Sources recovered by Source Extractor circled in red.

A. Blending

An issue that often arises with the recovery of dense dwarf galaxies is the overlapping of light, or blending, between resolved stars near the central region of the dwarf. We wished to explore this issue as part of another project searching for distant dwarf galaxies in DES Y6 data, but since the methods and data used are very similar to those used in our DELVE-DEEP dwarf detection tests, the results we found apply to this work as well. In order to characterize the effects of blending, 175 artificial dwarf galaxies with magnitudes $-8 \geq M_V \geq -12$ and half-light radii $2 \leq \log(r_h) \leq 3$ (central stellar densities $0.01 \lesssim \rho_{cen} \lesssim 10$, defined as the density of stars with i-band mag < 27 within one half-light radius) were injected across 3 DES Y6 coadds, and upon recovery, the absolute magnitude of each dwarf was re-calculated using only the recovered stars (stars defined as sources with `EXTENDED_CLASS` $\leq 2 -$ see Section III B). Dwarfs whose recovered magnitudes dropped below the 50% detection efficiency limit for the DES Y6 dwarf search were classified as "undetectable." While our detection efficiency differs slightly than that of the DES Y6 search, the general trend still applies to our data, which is that, on average, dwarf galaxies with higher central densities saw more significant decreases in their absolute magnitude assembled from recovered stars, and therefore experienced greater flux loss due to blending (see Figure 2). The effects of this phenomenon are made clear in our dwarf sensitivity results, explained in more detail in Section IV.

B. Dwarf Search

The source catalogs outputted by Source Extractor for each of the 26 coadds containing injected dwarf galaxies were run through our dwarf-search pipeline in order to determine whether or not each artificial dwarf could be detected. The pipeline first selects the red-giant-branch (RGB) sources from a catalog, defined as those that lie within the RGB box shown in Figure 3. Then, we applied star-galaxy separation in order to filter out all of the sources that are not likely to be stars. This was done using the `EXTENDED_CLASS` parameter, defined as the sum of three Boolean conditions involving Source Extractor's `SPREAD_MODEL` and `SPREADERR_MODEL`:

$$\begin{aligned} &\texttt{EXTENDED\_CLASS} = \\ &\quad ((\texttt{SPREAD\_MODEL} + 3 * \texttt{SPREADERR\_MODEL}) > 0.005) \\ &+ ((\texttt{SPREAD\_MODEL} + \texttt{SPREADERR\_MODEL}) > 0.003) \\ &+ ((\texttt{SPREAD\_MODEL} - \texttt{SPREADERR\_MODEL}) > 0.003) \end{aligned} \tag{1}$$

`EXTENDED_CLASS` values of 0 correspond to high-confidence stars, 1 corresponds to likely stars, 2 corresponds to likely galaxies (but still possible stars), and 3 corresponds to high-confidence galaxies.[13] Since star-galaxy separation becomes more difficult with such faint sources, we chose to apply a more generous star-galaxy cut and defined stars as sources with `EXTENDED_CLASS` ≤ 2.

Using these selected sources that we have now defined as RGB stars, we created binned density maps with `binsize`

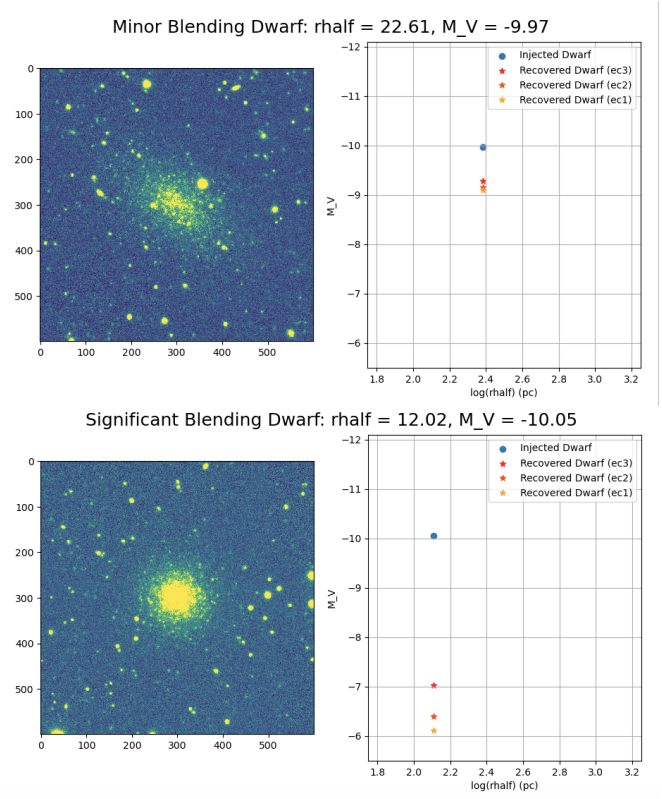

FIG. 2. Two images of artificial dwarf galaxies with their corresponding injected and recovered absolute magnitudes, one where blending does not have a significant effect (top), and one where it does (bottom). Injected mags given by blue circles, and recovered mags given by red, orange, and yellow stars. These three stars correspond to EXTENDED_CLASS ≤ 3 (no star-galaxy separation applied), EXTENDED_CLASS ≤ 2 (likely and unlikely stars), and EXTENDED_CLASS ≤ 1 (only likely stars), respectively.

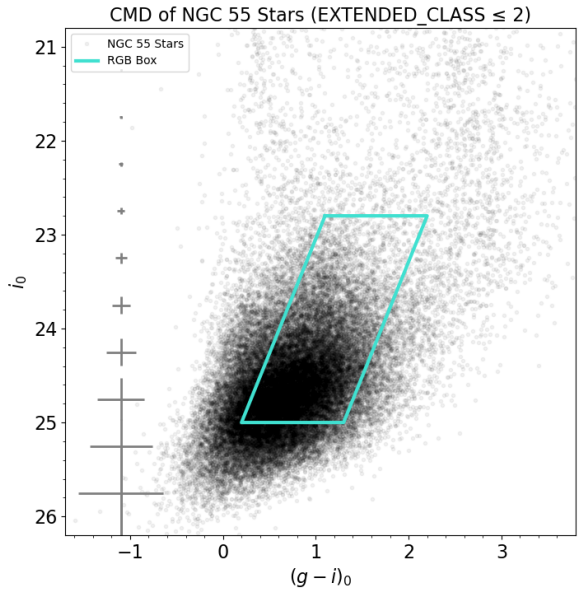

FIG. 3. g-i color vs. i-band magnitude for all stars (EXTENDED_CLASS ≤ 2) in the DELVE-DEEP NGC 55 footprint with the Red-Giant-Branch box plotted on top in turquoise. Magnitude error given by cross points on left.

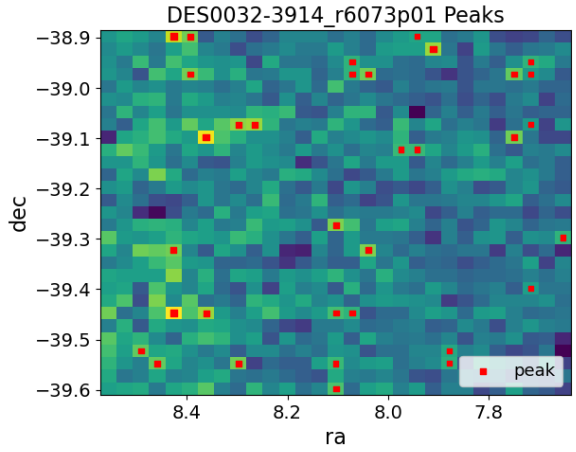

FIG. 4. Example of a density map for tile DES0032-3914 in the NGC 55 footprint, with binsize = 1.5 arcmin. Peaks identified by find_peaks given by red squares.

= 1.5 arcmin. To search for over-densities of RGB stars, we used the photutils function, find_peaks.[14] Depending on what parameters are used for find_peaks, different sets of dwarf galaxies can be detected, so in order to maximize our detection efficiency, we ran several iterations of find_peaks for each density map using different parameters and combined the results (see Figure 4). The first iteration of find_peaks was essentially a simple threshold test. The threshold for each bin in the density map was defined by MEDIAN_BKG + 3.0 * ST_DEV_BKG, where MEDIAN_BKG and ST_DEV_BKG are the median and standard deviation bin value of an annulus surrounding each bin. The find_peaks parameter, box_size, was set to 1, meaning each bin was looked at individually, and if its value was larger than its corresponding threshold value, then it was identified as a peak. The second iteration of find_peaks used a constant threshold for all bins in the density map, which was the median bin value across all bins. However, the box_size parameter was set to 7, meaning find_peaks looked within a region of size (7, 7) for each bin to search for peaks. If a bin containing an artificial dwarf was identified as a peak in either of these tests, then it was classified as a detection for that dwarf. In order to avoid the possibility of an injected dwarf being identified as a peak coincidentally, these two iterations of find_peaks were run on versions of all 26 coadds without injected dwarfs, and if any bin that normally contained an injected dwarf was identified as a peak in these tests, then that detection was not counted towards the total number of dwarf detections. After running this dwarf search on all 26 coadds and recording the detections, we determined our dwarf sensitivity by calculating the fraction of dwarfs that were detected within each size-luminosity bin, as seen in Figure 5.

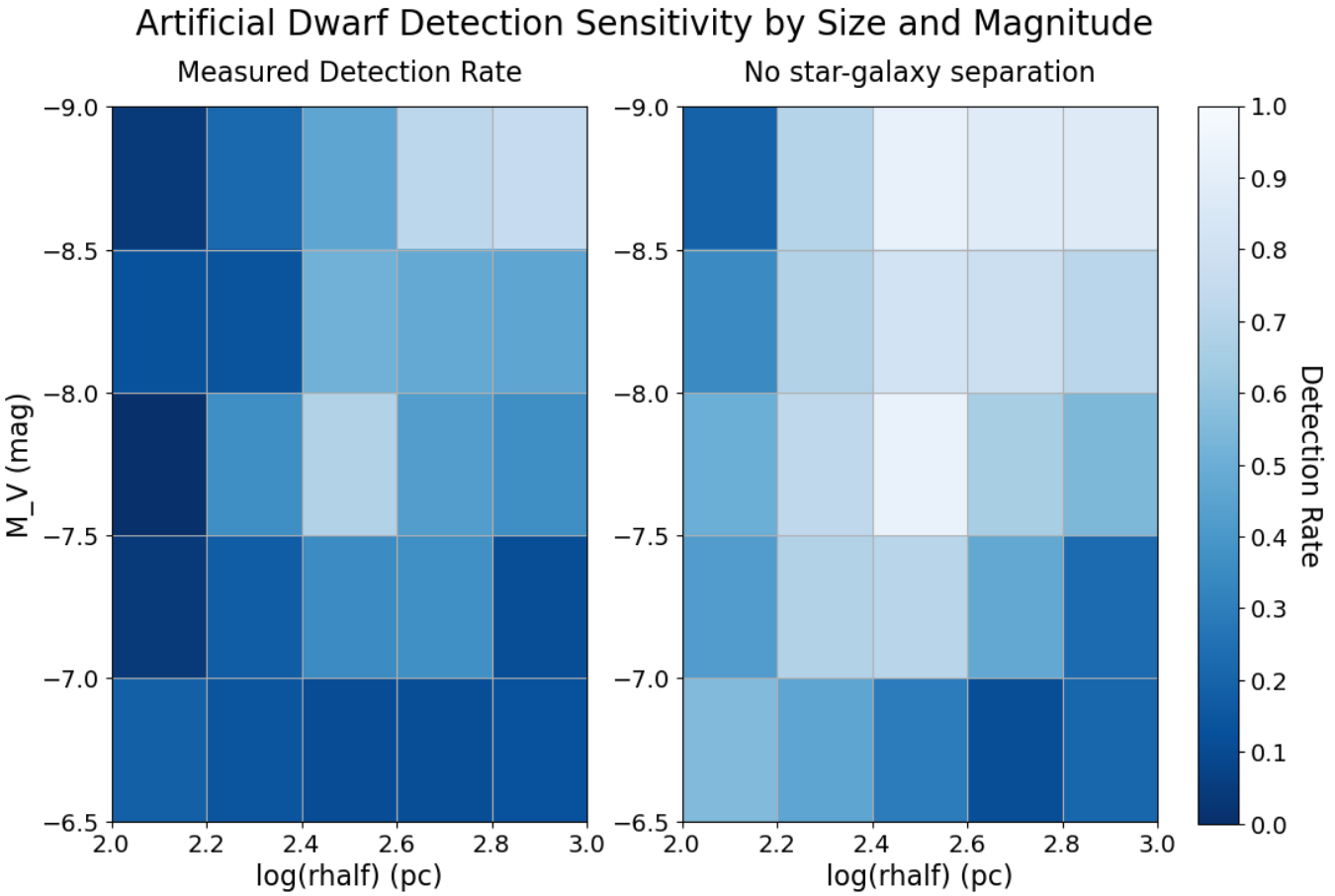

FIG. 5. Left: Measured detection sensitivity of injected artificial dwarf galaxies, given by the fraction of dwarfs that were detected within each size-luminosity bin. Right: Calculated detection sensitivity after not applying star-galaxy separation on the recovered dwarfs and re-running our dwarf-search pipeline.

IV. RESULTS

Our measured detection sensitivity for artificial dwarf galaxies, as well as the detection sensitivity calculated without applying star-galaxy separation, is given by Figure 5. Our measured results (left) show that for $M_V \lesssim -7.5$ and $\log(r_h) \gtrsim 2.4$, detection rates ranged from $0.5 - 0.7$ on average, and everywhere else, detection rates remained below $\sim$0.3. This trend reflects what we would expect based on DELVE-DEEP's detection limits and blending effects. DELVE-DEEP's expected detection limit is $M_V \sim -7$, so it makes sense that our measured detection rates start to drop around this magnitude. Additionally, our blending tests demonstrated that dwarfs with higher central densities experience greater flux loss upon recovery and would therefore be harder to detect, which is consistent with the lower detection rates we see for compact dwarfs with smaller half-light radii.

However, when compared to other dwarf sensitivity tests performed in recent years (e.g., Mutlu-Pakdil et al. 2021),[15] we would expect to see higher detection rates for dwarfs with $M_V \lesssim -7.0$ and $\log(r_h) \gtrsim 2.2$, as well as a smoother distribution with less random fluctuations. While this may be due in small part to not using enough artificial dwarfs and unoptimized `find_peaks` parameters, the main issue seems to come from the difficulties in performing star-galaxy separation for sources at this distance and magnitude. The right plot in Figure 5 shows the detection sensitivity calculated using the same `find_peaks` parameters, but without applying star-galaxy separation on the recovered dwarf sources, meaning all recovered dwarf sources were classified as stars and therefore were included in the final density map that was run through `find_peaks`. These results look much more similar to what we would expect in terms of detection rate values, with detection rates for the brightest, largest dwarfs ranging from $\sim 0.7-0.9$, and detection rates remaining relatively high for dwarfs with $M_V \lesssim -7.0$ and $\log(r_h) \gtrsim 2.2$. Additionally, this plot displays the trend of decreasing detection rates much more accurately. We still see the decrease in detection rate as magnitude becomes fainter than $M_V \sim -7$, but more specifically, we see a more significant decrease for diffuse, faint dwarfs. This makes sense, since it is harder to recover faint stars when they are spread out, as opposed to being clustered together. And similarly, we still see a decrease in detection rate as half-light radius decreases, but now we see that this

decrease primarily affects brighter compact dwarfs. This reflects the fact that the effects of blending are more significant for dwarfs with greater densities, not just those with smaller sizes.

A possible explanation for why star-galaxy separation proves to be difficult for these faint sources is illustrated by the example artificial dwarf shown in Figure 6. The segmentation map shows that many of the recovered sources for this dwarf are non-circular, which is the reason why so many of these sources are classified as galaxies (colored in red in the CMD). This suggests that stars that are injected near each other are being identified as one, elongated object rather than several, individual point sources. This reveals a type of blending different than that explored in Section III A, in that it affects clusters of stars on a much smaller scale and is not something that can easily be corrected for when detecting dwarf galaxies. It is also worth noting that the DELVE-DEEP PSF is relatively broad compared the PSF used in Mutlu-Pakdil et al. 2021,[15] and this PSF size has a major impact on the ability to accurately perform star-galaxy separation.

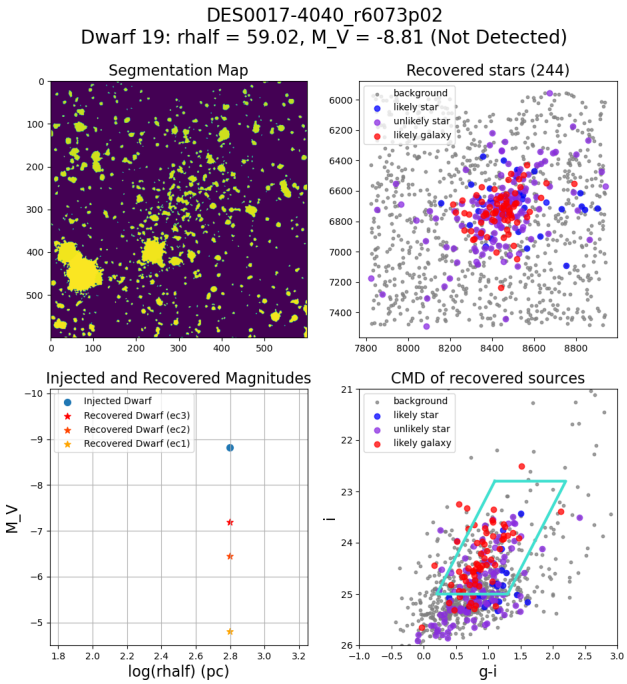

FIG. 6. Diagnostic plots for an artificial dwarf galaxy injected into tile DES0017-4040. Top-left: Segmentation map at the position of this injected dwarf. Top-right: Map of recovered and background sources at the position of this injected dwarf. Sources with EXTENDED_CLASS = 3 given in red, EXTENDED_CLASS = 2 given in purple, EXTENDED_CLASS $\leq$ 1 given in blue, and background stars given in gray. Bottom-left: Injected and recovered magnitudes of this dwarf. Injected mags given by blue circles, and recovered mags given by red, orange, and yellow stars, corresponding to EXTENDED_CLASS $\leq$ 3, 2, and 1, respectively. Bottom-right: Color magnitude diagram of recovered and background stars at the position of this injected dwarf, with same color scheme as top-right.

V. CONCLUSION

In this work, we measure the dwarf galaxy detection sensitivity of DELVE-DEEP NGC 55 data by injecting and recovering artificial dwarfs of varying size and luminosity. Our dwarf galaxies are modeled using a combination of point sources and Sérsic profiles and are injected across 26 coadded images from the DELVE-DEEP NGC 55 footprint. Sources are recovered by Source Extractor and the resulting catalogs are run through our dwarf-search pipeline, in which detections are identified using `find_peaks`. We also explore how the blending of resolved stars in dwarf galaxies affects their recovery by measuring the discrepancy between the injected and recovered absolute magnitude of dwarfs of varying central density.

Our results demonstrate that detection sensitivity is highest for large, bright dwarfs and begins to decrease for $M_V \gtrsim -7.5$ and $\log(r_h) \lesssim 2.4$. In other words, we are less sensitive to dwarf galaxies as we approach DELVE-DEEP's detection limit or the blending of resolved stars begins to cause significant flux loss upon recovery. Our results, however, were hampered by the fact that star-galaxy separation becomes increasingly difficult for distant, faint sources. Removing star-galaxy separation when calculating our detection sensitivity yields results that better match our expectations and more accurately illustrate the trends caused by our detection limit and blending. The inaccuracy of star-galaxy separation for these types of sources could be the result of the blending of small clusters of resolved stars that are identified as single, non-circular sources.

Looking ahead, we expect to run this dwarf-search pipeline on the entirety of DELVE-DEEP's real NGC 55 data, and the dwarf detection sensitivity that we measured in this work will tell us the sizes and luminosities of dwarf galaxies that we should be able to detect. Identifying any dwarf galaxy satellites that may exist around NGC 55 will allow us to place a constraint on the abundance of dwarf galaxies we expect to find around low-mass hosts, and ultimately, our goal will be to produce the first complete satellite luminosity function for a distant, MC-mass galaxy down to a limit of $M_V \sim -7$.

REFERENCES

[1] J. D. Simon, "The faintest dwarf galaxies," Annual Review of Astronomy and Astrophysics **57**, 375–415 (2019).

[2] J. D. Simon and M. Geha, "The Kinematics of the Ultra-faint Milky Way Satellites: Solving the Missing Satellite Problem," **670**, 313–331 (2007), arXiv:0706.0516 [astro-ph].

[3] A. W. McConnachie, "The Observed Properties of Dwarf Galaxies in and around the Local Group," **144**, 4 (2012), arXiv:1204.1562 [astro-ph.CO].

[4] D. J. Sand, K. Spekkens, D. Crnojević , J. R. Hargis, B. Willman, J. Strader, and C. J. Grillmair, "ANTLIA b: A FAINT DWARF GALAXY MEMBER OF THE NGC 3109 ASSOCIATION," The Astrophysical Journal **812**, L13 (2015).

[5] J. L. Carlin, D. J. Sand, P. Price, B. Willman, A. Karunakaran, K. Spekkens, E. F. Bell, J. P. Brodie, D. Crnojević , D. A. Forbes, J. Hargis, E. Kirby, R. Lupton, A. H. G. Peter, A. J. Romanowsky, and J. Strader, "FIRST RESULTS FROM THE MADCASH SURVEY: A FAINT DWARF GALAXY

COMPANION TO THE LOW-MASS SPIRAL GALAXY NGC 2403 AT 3.2 MPC," The Astrophysical Journal **828**, L5 (2016).

[6] J. L. Carlin, B. Mutlu-Pakdil, D. Crnojević, C. T. Garling, A. Karunakaran, A. H. G. Peter, E. Tollerud, D. A. Forbes, J. R. Hargis, S. Lim, A. J. Romanowsky, D. J. Sand, K. Spekkens, and J. Strader, "Hubble space telescope observations of two faint dwarf satellites of nearby lmc analogs from madcash*," The Astrophysical Journal **909**, 211 (2021).

[7] A. Drlica-Wagner, J. L. Carlin, D. L. Nidever, P. S. Ferguson, N. Kuropatkin, M. Adamó w, W. Cerny, Y. Choi, J. H. Esteves, C. E. Martínez-Vázquez, S. Mau, A. E. Miller, B. Mutlu-Pakdil, E. H. Neilsen, K. A. G. Olsen, A. B. Pace, A. H. Riley, J. D. Sakowska, D. J. Sand, L. Santana-Silva, E. J. Tollerud, D. L. Tucker, A. K. Vivas, E. Zaborowski, A. Zenteno, T. M. C. Abbott, S. Allam, K. Bechtol, C. P. M. Bell, E. F. Bell, P. Bilaji, C. R. Bom, J. A. Carballo-Bello, D. Crnojević, M.-R. L. Cioni, A. Diaz-Ocampo, T. J. L. de Boer, D. Erkal, R. A. Gruendl, D. Hernandez-Lang, A. K. Hughes, D. J. James, L. C. Johnson, T. S. Li, Y.-Y. Mao, D. Martínez-Delgado, P. Massana, M. McNanna, R. Morgan, E. O. Nadler, N. E. D. Noël, A. Palmese, A. H. G. Peter, E. S. Rykoff, J. Sánchez, N. Shipp, J. D. Simon, A. Smercina, M. Soares-Santos, G. S. Stringfellow, K. Tavangar, R. P. van der Marel, A. R. Walker, R. H. Wechsler, J. F. Wu, B. Yanny, M. Fitzpatrick, L. Huang, A. Jacques, R. Nikutta, and A. Scott, "The DECam local volume exploration survey: Overview and first data release," The Astrophysical Journal Supplement Series **256**, 2 (2021).

[8] G. A. Dooley, A. H. G. Peter, J. L. Carlin, A. Frebel, K. Bechtol, and B. Willman, "The predicted luminous satellite populations around SMC- and LMC-mass galaxies - a missing satellite problem around the LMC?" **472**, 1060–1073 (2017), arXiv:1703.05321 [astro-ph.GA].

[9] G. A. Dooley, A. H. G. Peter, T. Yang, B. Willman, B. F. Griffen, and A. Frebel, "An observer's guide to the (Local Group) dwarf galaxies: predictions for their own dwarf satellite populations," Monthly Notices of the Royal Astronomical Society **471**, 4894–4909 (2017).

[10] E. E. Salpeter, "The Luminosity Function and Stellar Evolution." **121**, 161 (1955).

[11] B. Rowe, M. Jarvis, R. Mandelbaum, G. M. Bernstein, J. Bosch, M. Simet, J. E. Meyers, T. Kacprzak, R. Nakajima, J. Zuntz, H. Miyatake, J. P. Dietrich, R. Armstrong, P. Melchior, and M. S. S. Gill, "Galsim: The modular galaxy image simulation toolkit," (2015), arXiv:1407.7676 [astro-ph.IM].

[12] E. Bertin and S. Arnouts, "SExtractor: Software for source extraction." **117**, 393–404 (1996).

[13] A. Drlica-Wagner, P. S. Ferguson, M. Adamów, M. Aguena, S. Allam, F. Andrade-Oliveira, D. Bacon, K. Bechtol, E. F. Bell, E. Bertin, P. Bilaji, S. Bocquet, C. R. Bom, D. Brooks, D. L. Burke, J. A. Carballo-Bello, J. L. Carlin, A. Carnero Rosell, M. Carrasco Kind, J. Carretero, F. J. Castander, W. Cerny, C. Chang, Y. Choi, C. Conselice, M. Costanzi, D. Crnojević, L. N. da Costa, J. de Vicente, S. Desai, J. Esteves, S. Everett, I. Ferrero, M. Fitzpatrick, B. Flaugher, D. Friedel, J. Frieman, J. García-Bellido, M. Gatti, E. Gaztanaga, D. W. Gerdes, D. Gruen, R. A. Gruendl, J. Gschwend, W. G. Hartley, D. Hernandez-Lang, S. R. Hinton, D. L. Hollowood, K. Honscheid, A. K. Hughes, A. Jacques, D. J. James, M. D. Johnson, K. Kuehn, N. Kuropatkin, O. Lahav, T. S. Li, C. Lidman, H. Lin, M. March, J. L. Marshall, D. Martínez-Delgado, C. E. Martínez-Vázquez, P. Massana, S. Mau, M. McNanna, P. Melchior, F. Menanteau, A. E. Miller, R. Miquel, J. J. Mohr, R. Morgan, B. Mutlu-Pakdil, R. R. Muñoz, E. H. Neilsen, D. L. Nidever, R. Nikutta, J. L. Nilo Castellon, N. E. D. Noël, R. L. C. Ogando, K. A. G. Olsen, A. B. Pace, A. Palmese, F. Paz-Chinchón, M. E. S. Pereira, A. Pieres, A. A. Plazas Malagón, J. Prat, A. H. Riley, M. Rodriguez-Monroy, A. K. Romer, A. Roodman, M. Sako, J. D. Sakowska, E. Sanchez, F. J. Sánchez, D. J. Sand, L. Santana-Silva, B. Santiago, M. Schubnell, S. Serrano, I. Sevilla-Noarbe, J. D. Simon, M. Smith, M. Soares-Santos, G. S. Stringfellow, E. Suchyta, D. J. Suson, C. Y. Tan, G. Tarle, K. Tavangar, D. Thomas, C. To, E. J. Tollerud, M. A. Troxel, D. L. Tucker, T. N. Varga, A. K. Vivas, A. R. Walker, J. Weller, R. D. Wilkinson, J. F. Wu, B. Yanny, E. Zaborowski, A. Zenteno, Delve Collaboration, Des Collaboration, and Astro Data Lab, "The DECam Local Volume Exploration Survey Data Release 2," **261**, 38 (2022), arXiv:2203.16565 [astro-ph.IM].

[14] Astropy Collaboration, T. P. Robitaille, E. J. Tollerud, P. Greenfield, M. Droettboom, E. Bray, T. Aldcroft, M. Davis, A. Ginsburg, A. M. Price-Whelan, W. E. Kerzendorf, A. Conley, N. Crighton, K. Barbary, D. Muna, H. Ferguson, F. Grollier, M. M. Parikh, P. H. Nair, H. M. Unther, C. Deil, J. Woillez, S. Conseil, R. Kramer, J. E. H. Turner, L. Singer, R. Fox, B. A. Weaver, V. Zabalza, Z. I. Edwards, K. Azalee Bostroem, D. J. Burke, A. R. Casey, S. M. Crawford, N. Dencheva, J. Ely, T. Jenness, K. Labrie, P. L. Lim, F. Pierfederici, A. Pontzen, A. Ptak, B. Refsdal, M. Servillat, and O. Streicher, "Astropy: A community Python package for astronomy," **558**, A33 (2013), arXiv:1307.6212 [astro-ph.IM].

[15] B. Mutlu-Pakdil, D. J. Sand, D. Crnojević, A. Drlica-Wagner, N. Caldwell, P. Guhathakurta, A. C. Seth, J. D. Simon, J. Strader, and E. Toloba, "Resolved dwarf galaxy searches within $\sim$5 mpc with the vera rubin observatory and subaru hyper suprime-cam*," The Astrophysical Journal **918**, 88 (2021).